PET imaging of Bronchoconstriction

We studied mild and moderate asthmatics in baseline and after bronchoconstriction provoked by inhalation of sufficient methacholine aerosol to reduce by 20% the forced expiratory volume in the first second (FEV1). The protocol was approved by the Massachusetts General Hospital Institutional Review Board. Dynamic PET images of 15 contiguous 6.5 mm thick cross-sections of the chest, with the subject lying supine, were acquired following an intravenous bolus injection of the positron-emitter Nitrogen-13 (^{13}NN) in saline solution during a short (20-30 sec) apnoea and a 3 minute period of washout during breathing. Due to its low solubility in water and blood (partition coefficient ~0.014), upon arrival at the pulmonary capillary bed, ^{13}NN diffuses into the alveoli and is later washed out in proportion to local ventilation. The Suppl. Videos illustrate, in a "hot" colour scale and modified time, the regional kinetics of the ^{13}NN tracer in an asthmatic subject in baseline (Suppl. Video S3) and after broncho-constriction by inhalation of methacholine (Suppl. Video S4). Note that in baseline, arrival of the ^{13}NN-saline bolus to the right heart is followed by a relatively uniform distribution of the tracer within the lung (with a concentration that is proportional to regional perfusion) and then by an almost complete removal of the tracer by the end of a washout period. In contrast, after bronchoconstriction, the distribution of the tracer (blood flow) is heterogeneous and followed by a substantially reduced washout from large contiguous "ventilation defects" encompassing a large fraction of the left lung and a smaller fraction of the right lung. A similar pattern of ventilation defects with large residual tracer is observed from a different subject (Suppl. Fig. S5 left). A three-dimensional rendering of the "ventilation defects" in this subject is shown in Fig. 1 of the paper.

At the end of the washout period the subject is asked to inhale deeply three times before imaging is continued for an additional period (Suppl. Fig. S5 right). Note that tracer removal by these deep inhalations is enhanced from certain parts of the defects and not from others.

Model of Bronchoconstriction in an Airway Tree

We developed a computational model of ventilation distribution in an airway tree with twelve generations (n = 12) of symmetric bifurcations. This tree has 8191 bronchial segments that can change their individual state as a result of interactions with their surrounding lung tissue. For generations $k = 0...11$, any bronchial segment is the parent of two daughter branches (a, b) shown in Fig. 1. The properties of such a self-similar branching pattern are best defined by recursive equations.

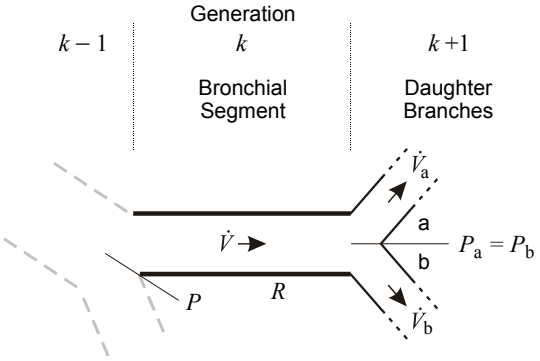

Figure 1 Flow ($\dot{V}$), pressure (P), and resistance (R) for the connected bronchial segments of two airway generations. The parameters of the connected branches at generation k+1 carry the index a or b to define the relations between the three bronchial segments. This definition is valid for all branching points of the tree.

The flow ($\dot{V}$) of breathing gases at time t through bronchial segment i at generation k is defined by

$$\dot{V}(t,k,i) = \dot{V}(t,k{+}1,i(\mathrm{a})) + \dot{V}(t,k{+}1,i(\mathrm{b}))$$

where i(a) is the index of the daughter branch a and i(b) of branch b at generation k+1. The inspired volume (V) associated to segment i at generation k from zero to t is

$$V(t,k,i) = \int_0^t \dot{V}(t,k,i)\,\mathrm{d}t + \mathrm{V}_0$$

The entrance pressure (P) of the bronchial segment is equal to the sum of the pressure at the daughter generation (k+1) and the pressure drop due to the airway resistance (R) when the flow goes through

$$P(t,k,i) = R(z,k,i)\ \dot{V}(t,k,i) + P(t,k{+}1,i(\mathrm{a}))$$

R is a function of the airway's length, radius (r) and gas viscosity, and is kept constant during an iteration step (z) equivalent to a breathing cycle of duration t_B ($z\ t_B \le t < (z{+}1)\ t_B$). The entrance pressures of the daughter branches a and b are equal

$$P(t,k{+}1,i(\mathrm{a})) = P(t,k{+}1,i(\mathrm{b}))$$

For the terminal generation k = n, P of the unit i is equal to the sum of pressures caused by airway resistance, by the compliance of lung parenchyma (C_L), and by the compliance of the chest wall (C_{cw})

$$P(t,\mathrm{n},i) = R(z,\mathrm{n},i)\ \dot{V}(t,\mathrm{n},i) + \frac{2^{\mathrm{n}}}{\mathrm{C_L}} \int_0^t \dot{V}(t,\mathrm{n},i)\,\mathrm{d}t + \frac{1}{\mathrm{C_{cw}}} \int_0^t \dot{V}(t,0,1)\,\mathrm{d}t$$

Note, the total volume into, or out of, the airway tree and thus, the volume change of the chest wall, is equal to the integral of flow trough the single bronchial segment at generation zero ($\dot{V}(t,0,1)$).
R increases during bronchoconstriction due to the decrease in airway radius (r). Any r is recalculated for each iteration z using a non-linear model of bronchial mechanics for bronchoconstriction[1]

$$r(z,k,i) = f(V(t,k,i), P(t,k,i), \tau_r)$$

We added the relative smooth muscle activation $\tau_r \in [0,1]$ to the model of bronchial mechanics to simulate activation levels between zero and maximal activation τ_{max} ($\tau = \tau_r\ \tau_{max}$). Fig. 2 shows an example of the non-linearity in the mechanics of a single terminal bronchiole during bronchoconstriction.

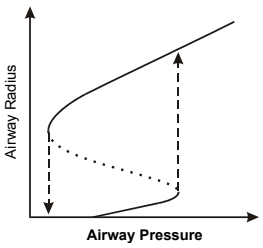

Figure 2 Example of the non-linearity generated by the model for a single terminal bronchiole at a high level of smooth muscle activation (1). For a range of entry airway pressures, the constricted bronchiole can take two stable states: severely constricted or open. Note that closing or opening of the bronchiole (arrows) leads to catastrophic shifts between these states and to hysteresis.

Equations are solved for conditions of cyclic breathing simulating constant tidal volume into the first branch of the tree with steady inspiratory flow rate and passive exhalation. Airway radii are iteratively adjusted to converge into steady values consistent with both the mechanics of the airway walls and the airflow distribution within the tree. To disrupt the numerical meta-stability of this uniform system, we introduce a small random heterogeneity (1% coefficient of variation) to airway wall thickness.

The spatial distribution of ventilation is displayed on a 64-by-64 grid of terminal units at the end of a Mandelbrot-like tree. The colour scale represents the mean-normalized ventilation of each unit. In the Suppl. Video S6 the model simulation involves a slow steady increase in smooth muscle relative

activation from 0 to 1.0 throughout the airway tree (bar at right hand corner) while tidal (breath) volume and breathing frequency are kept constant. The video is running on higher speed from zero to 0.8 of relative smooth muscle activation showing a stable ventilation distribution. Note the catastrophic formation of a large cluster (25% of the model) that enlarges in steps as smooth muscle activation increases. The histogram to the right demonstrates the conversion from a uniform and unimodal distribution of ventilation within the model to a highly heterogeneous and multimodal distribution that changes as the cluster covered areas increase with smooth muscle activation.

Suppl. Fig. S7 illustrates the complex dynamics of a random sample of 256 terminal units within the model for the simulation displayed in the Suppl. Video S6 as a function of smooth muscle activation level. Note the initial bifurcation at smooth muscle activation around 0.8 where a fraction of spatially correlated units (located in the left side of the lung model) begin to receive higher ventilation while the rest of the terminal units ventilation falls. As smooth muscle activation continues to increase, the terminal units losing ventilation get separated into distinct ventilation states in a series of additional bifurcations. With each of those bifurcations large groups of units catastrophically move towards virtual closure shifting ventilation towards units remaining open further increasing their ventilation. Each bifurcation is linked to a catastrophic increase in cluster size in the video (S6).

Suppl. Fig. S8 shows a step-wise reduction in cluster size (yellow) and the gradual reduction in the number of severely obstructed units (black) as tidal volume is increased while keeping smooth muscle activation and breathing frequency constant. The negative tidal volume dependency of cluster size is similar to that observed in the extent of the tracer retaining areas observed after deep inhalations in broncho-constricted asthmatics (Fig. 1a of paper and Suppl. Fig. S5).

Suppl. Fig. S9 shows the airway radius, normalized by the radius in the relaxed state, in each of the model's 12 generations for the conditions reached at the end of video S6. Lines connecting the data points show the pathways to each of the terminal units. Lines in red link airways within the cluster (right side of the model) and in blue airways outside the cluster. Note the clear separation between the two sides of the model and the 3 distinct levels of constriction in generation 12. Also important is to note that constriction of airways takes place at all levels of the tree (values of relative radii are less than unity) but it is clearly exaggerated in the airways leading to the cluster (points connected by red lines) and in particular in most of the airways leading to the highly constricted terminal bronchioles (generation 12 of the model).

Reference

1. Anafi RC, Wilson TA: Airway stability and heterogeneity in the constricted lung. J Appl Physiol 91: 1185-92, 2001